

This article was downloaded by:[Vanderbilt University]
[Vanderbilt University]

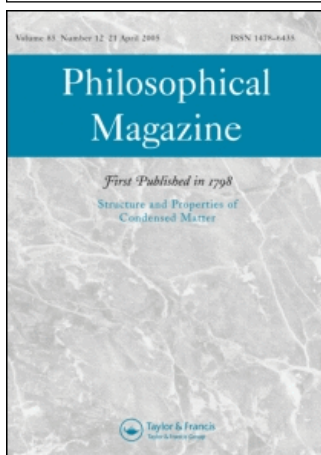
On: 23 May 2007

Access Details: [subscription number 731728355]

Publisher: Taylor & Francis

Informa Ltd Registered in England and Wales Registered Number: 1072954

Registered office: Mortimer House, 37-41 Mortimer Street, London W1T 3JH, UK



Philosophical Magazine

First published in 1798

Publication details, including instructions for authors and subscription information:
<http://www.informaworld.com/smpp/title-content=t713695589>

Surface composition effects on martensitic phase transformations in nickel aluminium nanowires

To cite this Article: Park, H. S. and Laohom, V. , 'Surface composition effects on martensitic phase transformations in nickel aluminium nanowires', Philosophical Magazine, 87:14, 2159 - 2168

To link to this article: DOI: 10.1080/14786430701199655

URL: <http://dx.doi.org/10.1080/14786430701199655>

PLEASE SCROLL DOWN FOR ARTICLE

Full terms and conditions of use: <http://www.informaworld.com/terms-and-conditions-of-access.pdf>

This article maybe used for research, teaching and private study purposes. Any substantial or systematic reproduction, re-distribution, re-selling, loan or sub-licensing, systematic supply or distribution in any form to anyone is expressly forbidden.

The publisher does not give any warranty express or implied or make any representation that the contents will be complete or accurate or up to date. The accuracy of any instructions, formulae and drug doses should be independently verified with primary sources. The publisher shall not be liable for any loss, actions, claims, proceedings, demand or costs or damages whatsoever or howsoever caused arising directly or indirectly in connection with or arising out of the use of this material.

© Taylor and Francis 2007

Surface composition effects on martensitic phase transformations in nickel aluminium nanowires

H. S. PARK* and V. LAOHOM

Department of Civil and Environmental Engineering, Vanderbilt University,
Nashville, TN 37235

(Received 24 November 2006; in final form 4 December 2006)

Atomistic simulations are utilized to quantify the effects of surface composition on stress-induced B2 to body centred tetragonal (BCT) martensitic phase transformations in intermetallic nickel aluminium (NiAl) nanowires. The simulations show that the phase transformation is observed in all considered cases, regardless of the material composition of the transverse {100} surfaces of the initially B2 wires. The results indicate that, for $\langle 100 \rangle$ oriented B2 wires with {100} transverse surfaces, the {100} orientation and not the material composition of the {100} surfaces is the dominant factor in controlling the ability of NiAl alloys to undergo martensitic phase transformations at nanometer scales.

1. Introduction

Metallic and semiconducting nanowires are now recognized as being among the most important building blocks for future nanotechnology-related developments. The proposed applications involving nanowires are far-reaching and interdisciplinary, including biosensors [1, 2], nanophotonic materials [3], interconnects in nanoscale circuitry [4], and many others [5].

Due to their diverse range of potential application, mechanical properties research has been performed to quantify the strength and failure characteristics of nanowires resulting from externally applied stresses and forces. This research has involved first principles calculations [6–8], molecular dynamics (MD) simulations [9–22], and experiment [23–27]. In general, the overall body of research has indicated that the nanowires are about one order of magnitude stronger than the corresponding bulk material, that the strength and failure characteristics are dependent on the crystallographic orientation of the nanowires, and that the deformation and post-yield behaviour is strain rate and temperature dependent.

Recently, several researchers have found using MD simulations that metal nanowires show unique structural reorientations and phase transformations that are not observed in the corresponding bulk materials. In particular, surface stresses were found to cause a face centred cubic (FCC) to body centred tetragonal (BCT) phase transformation in gold nanowires with cross-sectional features less than about

*Corresponding author. Email: harold.park@vanderbilt.edu

2 nm [28]. A reorientation from a $\langle 100 \rangle$ oriented wire to a $\langle 110 \rangle$ wire with $\{111\}$ low energy side surfaces was seen for larger single crystal monatomic FCC nanowires [19, 29–34]; the reorientation is possible due to the large surface stresses that exist on nanometer scale materials [35, 36]. Finally, the $\langle 110 \rangle / \{111\}$ nanowires were shown to exhibit both shape memory and pseudoelastic behaviour, marking their potential as self-healing nanoscale materials [30–33].

The phenomena of stress-induced martensitic phase transformations in nickel aluminium (NiAl) nanowires was recently observed for the first time [37]; the mechanical properties of the NiAl system including aspects of martensitic phase transformations have previously been studied by various researchers [38–52]. In [37], initially B2 nanowires were found to phase transform to a BCT phase by application of applied stress, which resulted in the propagation of $\{101\}$ -type twins and the resulting phase transformation. Due to the instability of the resulting BCT phase, the phase transformation was found to be reversible upon unloading, resulting in recoverable pseudoelastic strains of over 40 percent. The large recoverable pseudoelastic strains in both monatomic and alloyed nanowires far exceeds the 10 percent typically observed in bulk shape memory alloys such as nickel titanium (NiTi) [53].

The purpose of the present paper is to investigate the effects of surface composition on the stress-induced martensitic phase transformation in the NiAl nanowires. In particular, simulations were conducted on nanowires containing different combinations of nickel and aluminium $\{100\}$ surfaces. It is found that, for $\{100\}$ transverse surfaces and the $\langle 100 \rangle$ orientation, the disparate material surfaces do not degrade the ability of the NiAl nanowires to phase transform, thus adding additional merit to previous work on single crystal monatomic nanowires [19] indicating that the surface orientation, and not the material composition of the surfaces, may be the dominant factor in predicting and controlling the deformation characteristics of nanoscale materials.

2. Methods

The alloyed NiAl nanowires were created by generating atomic positions as in the bulk corresponding to the B2 crystal structure with a $\langle 100 \rangle$ orientation in the longitudinal x -direction. In this work, we considered four different cases of nanowires, which are illustrated in figure 1; all wires were initially in the B2 phase. The B2 crystal structure is an alloyed form of the traditional body centred cubic (BCC) lattice in which one material is found at the body centre, while the other material occupies the unit cell corners.

The nanowire cases are distinguished based on their surface composition; all surfaces correspond to $\{100\}$ planes of the B2 lattice, and are composed of either nickel or aluminium atoms. Cases I and IV contained only aluminium atoms on the surfaces; case I contained a total of 9874 atoms with a length of 15.498 nm in the x -direction, and had a square cross-section with length 2.583 nm in the y and z -directions. Case IV was a larger nanowire containing 42,103 atoms; its length was 25.106 nm in the x -direction, while having a square cross-section of lengths 4.305 nm in the y - and z -directions. The case I and IV wires were considered to investigate

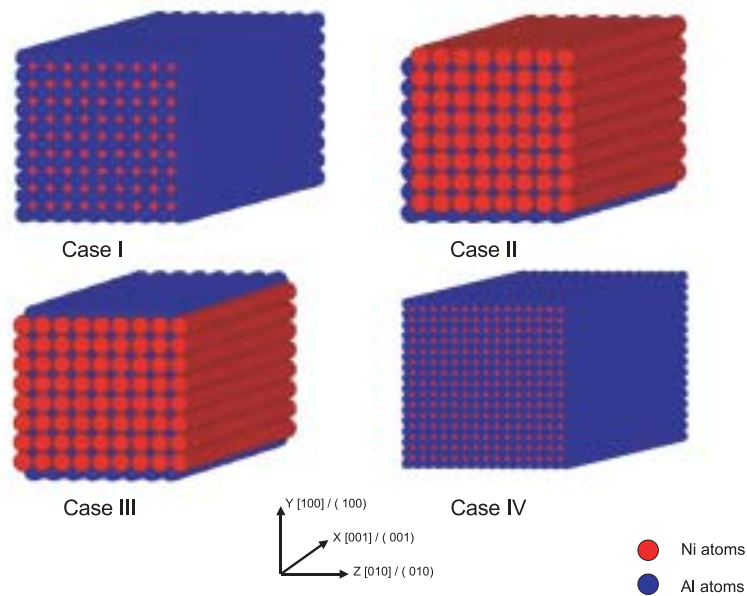


Figure 1. Schematic of the four cases of NiAl nanowires considered in this work.

whether utilizing a B2 structure with aluminium atoms at the unit cell corners with nickel in the centre prevented the stress-induced martensitic phase transformation from occurring.

The case II and III nanowires were created with both nickel and aluminium atoms on the surfaces as shown in figure 1. The case II wire contained 5760 atoms and had a length of 12.771 nm with a cross-sectional length of 2.009 nm, while the case III wire contained 6480 atoms and had a length of 12.828 nm with a cross-sectional length of 2.296 nm. The case II wire had two adjacent surfaces containing aluminium atoms, with the other two surfaces containing nickel; the case III wire had alternating nickel and aluminium surfaces. In all cases, the surface composition was different from that previously considered by Park [37]; the purpose of creating the wires with different surface compositions was to investigate whether the surface orientation or the material that constitutes the surface plays a larger role in controlling the martensitic phase transformation.

The lattice constant of the B2 structure was 0.28712 nm, and the NiAl alloy was modelled using the potential of Foiles [54], which is based on those developed by Voter and Chen [55, 56]. Off-stoichiometric compositions of NiAl, which have been utilized to increase the yield strength and hardening of polycrystalline NiAl alloys [38] are not considered in this work.

The NiAl nanowires were first relaxed to energy minimizing positions while keeping the ends of the wire constrained to move in the $\langle 100 \rangle$, or x -direction, then thermally equilibrated to 300 K using a Nosé–Hoover thermostat [57, 58]. The wires were then loaded in tension in the x -direction by fixing one end of the wire and applying a ramp velocity which went from zero at the fixed end to a maximum at the

loading end; the applied tensile strain rate was $\dot{\epsilon} \approx 10^9 \text{ s}^{-1}$. The purpose of the initial ramp velocity was to mitigate effects from shock loading that can occur in dynamic loading conditions. The tensile loading was performed adiabatically, or without thermostating. Finally, no periodic boundary conditions were used during any phase of the simulations, which were performed using the Sandia-developed code Warp [59, 60].

3. Results

3.1. Case I and IV nanowires

We first discuss the case I and IV nanowires. As discussed earlier, these wires were created in order to investigate a B2 lattice containing nickel atoms at the body centre with aluminium atoms at the unit cell corners; previous work on NiAl nanowires [37] considered a unit cell with aluminium at the body centre with nickel at the cell corners. In addition, the case IV wire was created to consider the effects of size on the martensitic phase transformation, as the shape memory and pseudoelasticity in single crystal, monatomic FCC nanowires was shown to be strongly dependent on surface stresses, which decrease with increasing wire size [19, 30–33].

Figure 2 illustrates the stress-induced martensitic phase transformation for the case I NiAl nanowires; similar behaviour including the martensitic phase transformation is observed for the case IV wires. The figure illustrates that the case I wire undergoes the phase transformation via the nucleation, propagation and annihilation of {101} twinning planes.

The microstructural details regarding the phase transformation can be correlated to the observed fluctuations and variations of the stress–strain response, as seen in figure 3. For both wires, the initially linear elastic deformation ceases at a strain of $\epsilon \approx 0.09$. At that point, a relaxation is observed followed by a period of constant stress. The relaxation corresponds to the initiation of the phase transformation from B2 to BCT by the nucleation of {101} twinning planes that sweep through the wire forming an interface between the initial B2 and resulting BCT phases. At a strain of $\epsilon \approx 0.3$, a second period of linear elastic deformation is observed, which corresponds to stretching of the fully BCT wire following completion of the phase transformation. The stress increases and relaxations between $\epsilon \approx 0.09$ and $\epsilon \approx 0.3$ correspond to the interaction and annihilation of the propagating twin boundaries.

The stress–strain curve in figure 3 also serves to illustrate the effects of size on the mechanical properties of the NiAl nanowires. The major differences are the values for the transformation stress (the stress at $\epsilon \approx 0.09$ when the phase transformation initiates), and the maximum stress that is supported by the BCT phase (the stress at $\epsilon \approx 0.42$ before strength loss due to irreversible yielding). The comparison gives 2.7 GPa/10.4 GPa for the case I wires versus 1.8 GPa/8.8 GPa for the case IV wires. In between these end points, the stress–strain behaviour of both wires is quite similar, indicating that the same mechanisms controlling the phase transformation are operative in both cases. This reduction in strength with increasing wire size is consistent with previous investigations of nanowire deformation [16, 20] indicating that a larger wire size leads to a smaller intrinsic surface stress barrier that needs to

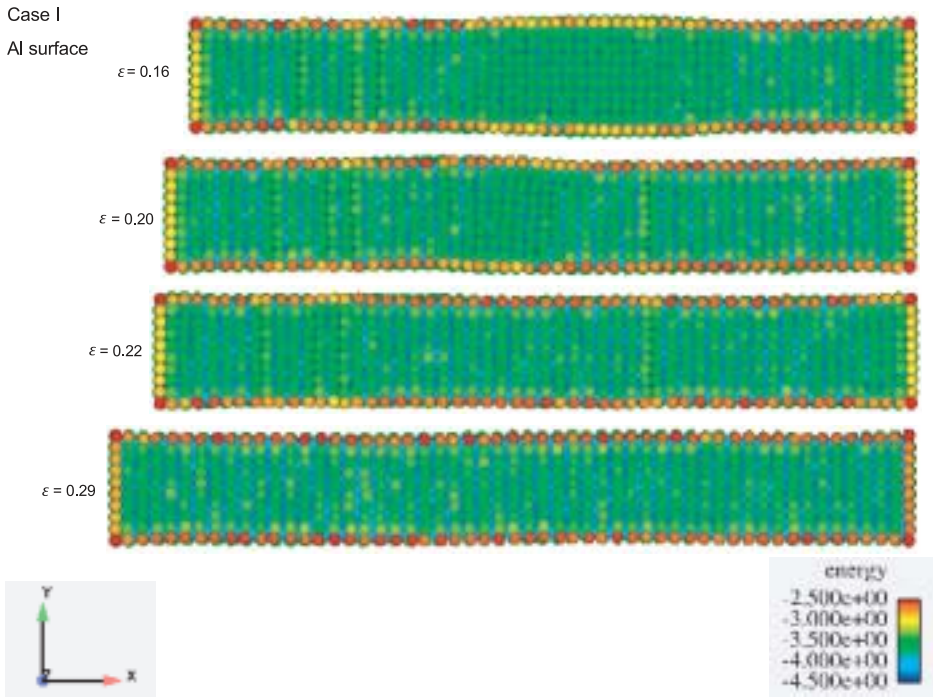


Figure 2. Stress-induced martensitic phase transformation for case I NiAl nanowire.

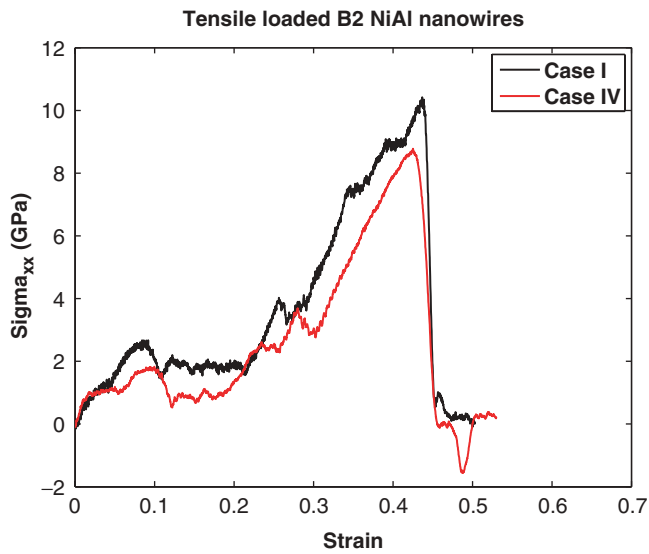


Figure 3. Stress-strain curves for case I and IV NiAl nanowires.

be overcome in order for yielding to occur, thus leading to reduced strength levels in the nanowire.

Another interesting result is obtained by comparing the mechanical properties of NiAl wires with Al surfaces, as is done in the present work, with NiAl wires with Ni surfaces, as was done by Park [37]; the comparison is shown in figure 4. As can be seen, the utilization of aluminium surfaces leads to transformation strains and peak strength levels that are more than double that achieved by the wire with nickel surfaces. While the eventual fracture strains appear to be similar, this example clearly illustrates the ability to tailor the mechanical properties and behaviour of nanoscale materials through surface engineering while maintaining the desired phase transformation characteristics.

3.2. Case II and III nanowires

We next discuss the phase transformation for the case II and III nanowires, or those wires with both nickel and aluminium atoms on the transverse {100} free surfaces. The phase transformation for the case II wire is shown in figure 5, while the transformation for the case III wire is shown in figure 6.

As can be seen in figures 5 and 6, both wires undergo the stress-induced martensitic phase transformation from B2 to BCT. The characteristics of the phase transformation are similar to that observed in the case I and IV nanowires, including the formation and propagation of {101} twinning planes which enable the transformation from B2 to BCT. In addition, the twin boundary propagation leads to localized bending in the wire, best seen in figure 5 at a strain of $\epsilon = 0.25$ and in figure 6 at a strain of $\epsilon = 0.26$. The various nickel and aluminium surfaces are seen to be relatively defect-free upon completion of the phase transformation, indicating that

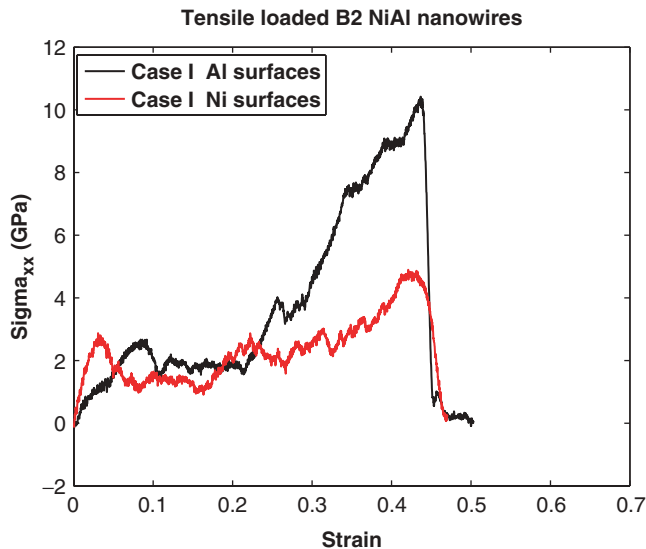


Figure 4. Stress-strain curves for NiAl wires with all aluminium or all nickel surfaces.

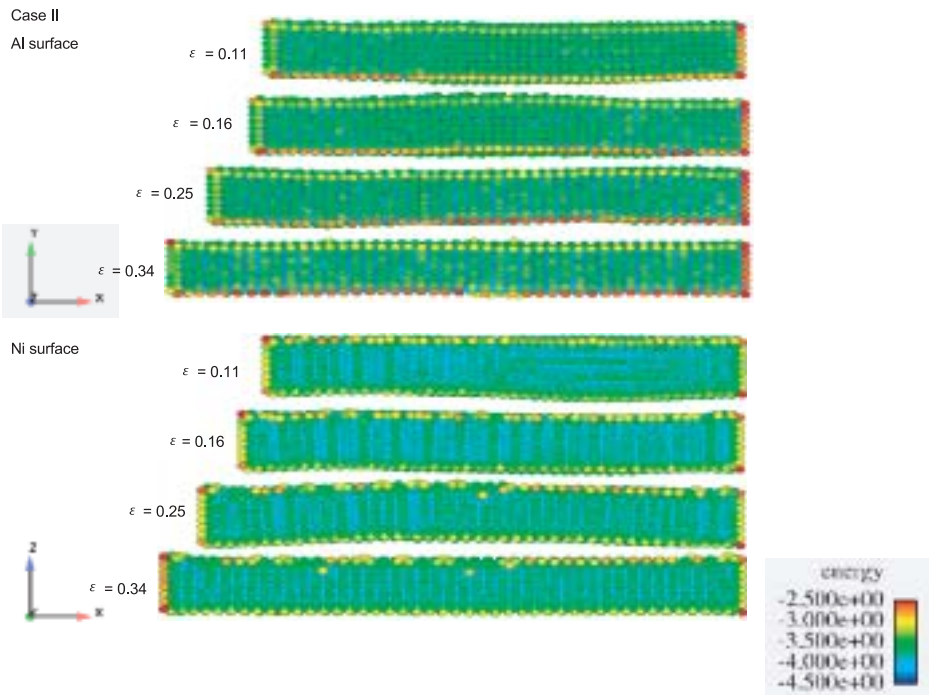


Figure 5. Stress-induced martensitic phase transformation for case II NiAl nanowire.

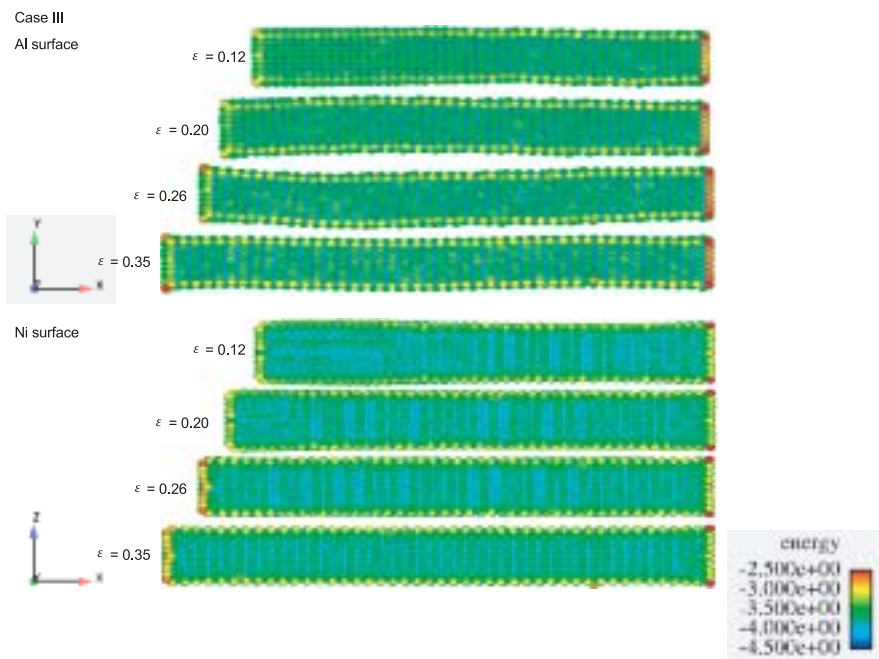


Figure 6. Stress-induced martensitic phase transformation for case III NiAl nanowire.

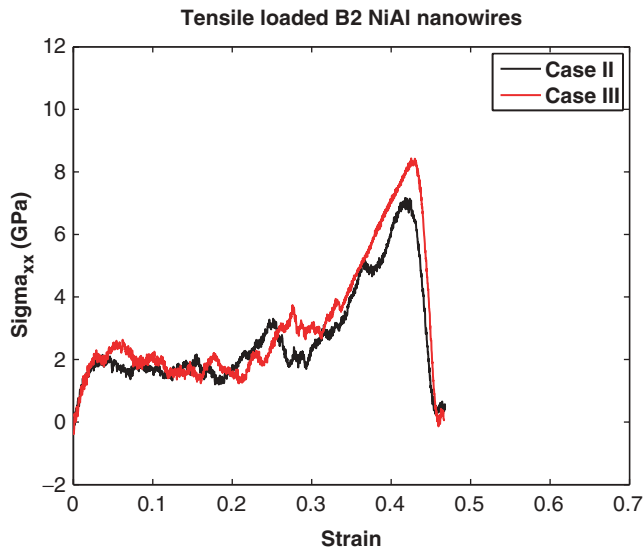


Figure 7. Stress–strain curves for case II and III nanowires.

the relative mismatch in nickel and aluminium surface stresses [61] does not cause inhomogeneous surface deformations that hinder the phase transformation.

The stress–strain curves for the case II and III nanowires are shown in figure 7. Both wires show a similar transformation stress of about 2 GPa at a strain level of about $\epsilon = 0.02$. The stress plateau then remains relatively constant until a strain level of about $\epsilon = 0.2$ is reached, at which point the stress begins to increase in both wires. The relaxations observed in both wires, but most prominently for the case III wire at a strain level of $\epsilon = 0.25$ are due to the annihilation of the $\{101\}$ twins which form due to distinct B2 and BCT phases in the wires. The localized stress peaks occur due to the effort necessary to transform discrete portions of the wire to the BCT phase; the subsequent relaxation occurs once the BCT phase is formed. The phase transformation between B2 and BCT phases is complete in both case II and III wires at a strain of $\epsilon \approx 0.31$, at which point a second linearly elastic period of deformation is observed in figure 7.

Comparing the strength levels achieved by the case II and III wires with those achieved by the case I and IV wires further illustrates the effect of engineering the mechanical properties of the nanowires by the material composition of the transverse free surfaces. Interestingly, the case II and III wires show a similar tangent modulus during the elastic stretching of the resulting BCT phase; this period of elongation occurs between strain levels of $\epsilon \approx 0.31$ and $\epsilon \approx 0.42$ as shown in figure 7. This implies that the elastic strength of the BCT phase is more strongly affected by the fact that both case II and case III wires have two nickel $\{100\}$ and two aluminium $\{100\}$ surfaces than due to the interactions of the adjacent nickel and aluminium surfaces. Both case II and III wires, which have a combination of nickel and aluminium free surfaces, also show reduced maximum strength (< 8 GPa) as compared to the case I wire (10.4 GPa). Due to the similarity in

wire size, this reduction in strength is clearly caused by the incorporation of nickel atoms on the transverse free surfaces.

4. Conclusions

We have utilized atomistic simulations to study specific aspects of the stress-induced martensitic phase transformation in intermetallic nickel aluminium (NiAl) nanowires. The simulations focused on investigating whether nanowire size or surface composition deleteriously affected the ability of the NiAl nanowires to undergo a martensitic phase transformation. In particular, the key finding of this work is that the surface composition of the nanowires does not appear to deleteriously affect the phase transformation. This was demonstrated by creating the nanowires with different materials on the {100} transverse surfaces of the initially B2 wires. For the systems considered, the nanowires did not appear to be size-limited in exhibiting the stress-induced phase transformation.

All wires considered in this work were observed to phase transform from the initial B2 phase to the resultant BCT phase via the same deformation mechanism; the mechanism observed was the initiation, propagation and annihilation of {101} twinning planes. However, it was clearly shown that the mechanical properties of the phase transforming wires, such as transformation strains and maximum strength, could be dramatically altered simply by changing the material composition of the transverse free surfaces. We note also that different surface terminations for the $\langle 100 \rangle$ oriented B2 phase were not considered in this work; however, previous research [19, 22] has indicated that both the surface orientation as well as geometry can have a first order effect on the observed nanowire deformation modes. Future research should, in conjunction with experimental data that reveals the commonly observed surface terminations of B2 NiAl wires, focus on quantifying these effects on the phase transforming ability of NiAl at nanometer length scales.

Acknowledgment

HSP acknowledges startup funding from Vanderbilt University in support of this research. VL acknowledges support from a National Science Foundation Graduate Research Fellowship.

References

- [1] C.M. Lieber, MRS Bull. **28**(7) 486 (2003).
- [2] P. Yang, MRS Bull. **30**(2) 85 (2005).
- [3] L.T. Canham, Appl. Phys. Lett. **57**(10) 1046 (1990).
- [4] N.I. Kovtyukhova and T.E. Mallouk, Chem. – A Eur. J. **8**(9) 4355 (2002).
- [5] Y. Xia, P. Yang, Y. Sun, *et al.*, Adv. Mater. **15**(5) 353 (2003).
- [6] H. Mehrez and S. Ciraci, Phys. Rev. B **56**(19) 12632 (1997).
- [7] D. Sanchez-Portal, E. Artacho, J. Junquera, *et al.*, Phys. Rev. Lett. **83**(19) 3884 (1999).
- [8] E.Z. da Silva, A.J.R. da Silva, and A. Fazzio, Phys. Rev. Lett. **87**(25) 256102 (2001).
- [9] H. Ikeda, Y. Qi, T. Cagin, *et al.*, Phys. Rev. Lett. **82**(14) 2900 (1999).
- [10] U. Landman, W.D. Luedtke, N.A. Burnham, *et al.*, Science **248** 454 (1990).

- [11] P.S. Branicio and J.P. Rino, *Phys. Rev. B* **62**(24) 16950 (2000).
- [12] P. Walsh, W. Li, R.K. Kalia, *et al.*, *Appl. Phys. Lett.* **78**(21) 3328 (2001).
- [13] J.-W. Kang and H.-J. Hwang, *Nanotechnology* **12** 295 (2001).
- [14] H.A. Wu, A.K. Soh, X.X. Wang, *et al.*, *Key Eng. Mater.* **261–263** 33 (2004).
- [15] W. Liang and M. Zhou, in *Proceedings of the Institution of Mechanical Engineers, Part C: Journal of Mechanical Engineering Science*, Vol. 218, pp. 599–606 (2004).
- [16] K. Gall, J. Diao and M.L. Dunn, *Nano Lett.* **4**(12) 2431 (2004).
- [17] J. Diao, K. Gall and M.L. Dunn, *Nano Lett.* **4**(10) 1863 (2004).
- [18] P.Z. Coura, S.G. Legoas, A.S. Moreira, *et al.*, *Nano Lett.* **4**(7) 1187 (2004).
- [19] H.S. Park, K. Gall and J.A. Zimmerman, *J. Mech. Phys. Solids* **54**(9) 1862 (2006).
- [20] H.S. Park and J.A. Zimmerman, *Phys. Rev. B* **72** 054106 (2005).
- [21] H.S. Park and J.A. Zimmerman, *Scripta Mater.* **54**(6) 1127 (2006).
- [22] C. Ji and H.S. Park, *Appl. Phys. Lett.* **89** 181916 (2006).
- [23] E.W. Wong, P.E. Sheehan and C.M. Lieber, *Science* **277** 1971 (1997).
- [24] P.E. Marszalek, W.J. Greenleaf, H. Li, *et al.*, in *Proceedings of the National Academy of Science*, Vol. 97, pp. 6282–6286 (2000).
- [25] B. Wu, A. Heidelberg and J.J. Boland, *Nature Mater.* **4** 525 (2005).
- [26] S. Cuenot, C. Frétygny, S. Demoustier-Champagne, *et al.*, *Phys. Rev. B* **69** 165410 (2004).
- [27] G.Y. Jing, H.L. Duan, X.M. Sun, *et al.*, *Phys. Rev. B* **73** 235409 (2006).
- [28] J. Diao, K. Gall and M.L. Dunn, *Nature Mater.* **2**(10) 656 (2003).
- [29] J. Diao, K. Gall and M.L. Dunn, *Phys. Rev. B* **70** 075413 (2004).
- [30] W. Liang and M. Zhou, *J. Eng. Mater. Techn.* **127**(4) 423 (2005).
- [31] W. Liang, M. Zhou and F. Ke, *Nano Lett.* **5**(10) 2039 (2005).
- [32] H.S. Park, K. Gall and J.A. Zimmerman, *Phys. Rev. Lett.* **95** 255504 (2005).
- [33] H.S. Park and C. Ji, *Acta Mater.* **54**(10) 2645 (2006).
- [34] W. Liang and M. Zhou, *Phys. Rev. B* **73** 115409 (2006).
- [35] R.C. Cammarata, *Prog. Surf. Sci.* **46**(1) 1 (1994).
- [36] W. Haiss, *Reports Prog. Phys.* **64** 591 (2001).
- [37] H.S. Park, *Nano Lett.* **6**(5) 958 (2006).
- [38] E.P. George, M. Yamaguchi, K.S. Kumar, *et al.*, *Annual Rev. Mater. Sci.* **24** 409 (1994).
- [39] E.P. George, C.T. Liu, J.A. Horton, *et al.*, *Mater. Characteri.* **39** 665 (1997).
- [40] K.K. Jee, P.L. Potapov, S.Y. Song, *et al.*, *Scripta Mater.* **36**(2) 207 (1997).
- [41] A. Nagasawa, K. Enami, Y. Ishino, *et al.*, *Scripta Metallurg.* **8** 1055 (1974).
- [42] Y.D. Kim and C.M. Wayman, *Scripta Metallurg. Mater.* **24**(2) 245 (1990).
- [43] S. Rubini and P. Ballone, *Phys. Rev. B* **48**(1) 99 (1993).
- [44] Y.Y. Ye, C.T. Chan, K.M. Ho, *et al.*, *Phys. Rev. B* **49**(9) 5852 (1994).
- [45] Y. Shao, P.C. Clapp and J.A. Rifkin, *Metallurg. Mater. Trans. A*, **27A** 1477 (1996).
- [46] R. Meyer and P. Entel, *Comput. Mater. Sci.* **10** 10 (1998).
- [47] T. Li, J.W. Morris and D.C. Chrzan, *Phys. Rev. B* **70** 054107 (2004).
- [48] D. Farkas, B. Mutasa, C. Vailhe, *et al.*, *Modell. Simul. Mater. Sci. Eng.* **3** 201 (1995).
- [49] V. Paidar, L.G. Wang, M. Söb, *et al.*, *Modell. Simul. Mater. Sci. Eng.* **7** 369 (1999).
- [50] M. Söb, L.G. Wang and V. Vitek, *Comput. Mater. Sci.* **8** 100 (1997).
- [51] M. Ludwig and P. Gumbsch, *Modell. Simul. Mater. Sci. Eng.* **3** 533 (1995).
- [52] R. Schroll, V. Vitek and P. Gumbsch, *Acta Mater.* **46**(3) 903 (1998).
- [53] K. Otsuka and X. Ren, *Prog. Mater. Sci.* **50** 511 (2005).
- [54] S.M. Foiles and M.S. Daw, *J. Mater. Res.* **2**(1) 5 (1987).
- [55] S.P. Chen, A.F. Voter and D.J. Srolovitz, *Phys. Rev. Lett.* **57**(11) 1308 (1986).
- [56] A.F. Voter and S.P. Chen, in *Accurate Interatomic Potentials For Ni, Al and Ni₃Al, Materials Research Society Symposium Proceedings*, Vol. 82 pp. 175–180 (1987).
- [57] S. Nosé, *J. Chem. Phys.* **81** 511 (1984).
- [58] W.G. Hoover, *Phys. Rev. A* **31** 1695 (1985).
- [59] S.J. Plimpton, *J. Comput. Phys.* **117** 1 (1995).
- [60] Warp. <http://www.cs.sandia.gov/~sjplimp/lammps.html> (2006).
- [61] J. Wan, Y.L. Fan, D.W. Gong, *et al.*, *Model. Simul. Mater. Sci. Eng.* **7** 189 (1999).